Journal of Zhejiang University-SCIENCE B (Biomedicine & Biotechnology)
ISSN 1673-1581 (Print); ISSN 1862-1783 (Online)
www.jzus.zju.edu.cn; www.springerlink.com
E-mail: jzus@zju.edu.cn

# RGFP966 inactivation of the YAP pathway attenuates cardiac dysfunction induced by prolonged hypothermic preservation*

Xiao-he ZHENG[1], Lin-lin WANG[1,2], Ming-zhi ZHENG[3], Jin-jie ZHONG[1,4], Ying-ying CHEN[†‡1,4], Yue-liang SHEN[†‡1]

[1]*Department of Basic Medicine Sciences, Zhejiang University School of Medicine, Hangzhou 310058, China*

[2]*Department of Orthopaedics, Sir Run Run Shaw Hospital, Zhejiang University School of Medicine, Hangzhou 310016, China*

[3]*Department of Pharmacology, Hangzhou Medical College, Hangzhou 310053, China*

[4]*Department of Obstetrics, the Second Affiliated Hospital, Zhejiang University School of Medicine, Hangzhou 310009, China*

[†]E-mail: bchenyy@zju.edu.cn; shenyueliang@zju.edu.cn

Received Jan. 21, 2020; Revision accepted May 11, 2020; Crosschecked Aug. 11, 2020

**Abstract:** Oxidative stress and apoptosis are the key factors that limit the hypothermic preservation time of donor hearts to within 4–6 h. The aim of this study was to investigate whether the histone deacetylase 3 (HDAC3) inhibitor RGFP966 could protect against cardiac injury induced by prolonged hypothermic preservation. Rat hearts were hypothermically preserved in Celsior solution with or without RGFP966 for 12 h followed by 60 min of reperfusion. Hemodynamic parameters during reperfusion were evaluated. The expression and phosphorylation levels of mammalian STE20-like kinase-1 (Mst1) and Yes-associated protein (YAP) were determined by western blotting. Cell apoptosis was measured by the terminal deoxynucleotidyl-transferase (TdT)-mediated dUTP nick-end labeling (TUNEL) method. Addition of RGFP966 in Celsior solution significantly inhibited cardiac dysfunction induced by hypothermic preservation. RGFP966 inhibited the hypothermic preservation-induced increase of the phosphorylated (p)-Mst1/Mst1 and p-YAP/YAP ratios, prevented a reduction in total YAP protein expression, and increased the nuclear YAP protein level. Verteporfin (VP), a small molecular inhibitor of YAP–transcriptional enhanced associate domain (TEAD) interaction, partially abolished the protective effect of RGFP966 on cardiac function, and reduced lactate dehydrogenase activity and malondialdehyde content. RGFP966 increased superoxide dismutase, catalase, and glutathione peroxidase gene and protein expression, which was abolished by VP. RGFP966 inhibited hypothermic preservation-induced overexpression of B-cell lymphoma protein 2 (Bcl-2)-associated X (Bax) and cleaved caspase-3, increased Bcl-2 mRNA and protein expression, and reduced cardiomyocyte apoptosis. The antioxidant and anti-apoptotic effects of RGFP966 were cancelled by VP. The results suggest that supplementation of Celsior solution with RGFP966 attenuated prolonged hypothermic preservation-induced cardiac dysfunction. The mechanism may involve inhibition of oxidative stress and apoptosis via inactivation of the YAP pathway.

**Key words:** Hypothermic preservation; RGFP966; Yes-associated protein (YAP); Oxidative stress; Apoptosis
https://doi.org/10.1631/jzus.B2000026 **CLC number:** R331.3

## 1 Introduction

Heart transplantation is a major strategy to improve the quality of life and prolong survival of patients with end-stage heart failure (Mehra et al., 2016). Donor hearts are typically hypothermically preserved in preparation for transplantation. Oxidative stress and apoptosis are the key factors that lead

‡ Corresponding authors
* Project supported by the National Natural Science Foundation of China (No. 81871541)
ORCID: Ying-ying CHEN, https://orcid.org/0000-0003-4054-884X; Yue-liang SHEN, https://orcid.org/0000-0002-6110-1329

to cardiomyocyte injury in hypothermically preserved hearts (Korkmaz-Icöz et al., 2019), which restricts their preservation time to within 4–6 h. Therefore, to prolong their preservation time and enhance the source of donor hearts, alleviation of prolonged hypothermic preservation-induced oxidative stress and inhibition of apoptosis would be appropriate goals.

Histone deacetylase (HDAC) inhibitors have been proven to protect against cardiac injury during different cardiovascular conditions. Pan-HDAC inhibitors can improve cardiac function in heart failure animal models. The improvement is associated with attenuation of oxidative stress and inflammation, and improvement of cardiac metabolism (McKinsey, 2012; Lkhagva et al., 2015). Inhibition of class I HDAC restored left ventricular contractile function in isolated ischemia-reperfusion rat hearts by increasing mitochondrial superoxide dismutase (SOD) and catalase (CAT) expression (Aune et al., 2014). HDAC3 is a key regulator of cell proliferation during cardiac development (Poleshko et al., 2017), and plays an important role in maintaining myocardial energy metabolism, cardiac electrophysiological property, and contractile function (Ferguson and McKinsey, 2015; Brundel et al., 2020). RGFP966 is a selective inhibitor of HDAC3 and is a more efficient inhibitor than other class I HDAC inhibitors (Malvaez et al., 2013). Janczura et al. (2018) reported that RGFP966 decreased Tau phosphorylation and Aβ-42 protein expression in the brain, and improved spatial learning and memory in an Alzheimer's disease mouse model. RGFP966 can also prevent diabetes-induced liver damage and cardiac injury, and ameliorate cerebral ischemia reperfusion injury in diabetic animal models (Xu et al., 2017; Zhang J et al., 2018; Zhao et al., 2019). In an experimental model of atrial fibrillation, RGFP966 delayed progression of atrial fibrillation and preserved contractile function (Zhang DL et al., 2018). Antioxidant and anti-apoptosis properties of RGFP966 have also been reported in animal models of optic nerve injury (Schmitt et al., 2018) and acute lung injury (Joshi et al., 2015). So we hypothesized that RGFP966 might have potential for the alleviation of cardiac dysfunction induced by hypothermic preservation.

Recent studies have demonstrated that HDAC inhibitors can alleviate oxidative stress (Yu et al., 2018), regulate inflammation response (Rivera-Reyes et al., 2018), manipulate cell cycle (Ren et al., 2019), and inhibit apoptosis (Jung et al., 2017) by targeting the Hippo pathway. The Yes-associated protein (YAP) and its homolog transcriptional coactivator with PDZ-binding motif (TAZ) are the key downstream effectors of the Hippo pathway (Li et al., 2018; Fu et al., 2019). When the Hippo pathway is inactive, YAP/TAZ is dephosphorylated and imported into the nucleus. In the nucleus, YAP/TAZ binds to transcriptional enhanced associate domains (TEADs), and then promotes gene transcription. HDAC8 has been reported to enhance the migration of breast cancer cells by activating Hippo-YAP signals (An et al., 2019). Overexpression of HDAC3 caused a significant increase in TEAD4 expression and resulted in negative regulation of Schwann cell myelination (Rivera-Reyes et al., 2018).

In the present study, we aimed to investigate whether RGFP966 could protect against prolonged hypothermic preservation-induced cardiac injury, and explored the role of Hippo-YAP signaling in hypothermically preserved rat hearts.

## 2 Materials and methods

### 2.1 Animals

Male Sprague-Dawley rats (each weighing 250–300 g) were purchased from the Experimental Animal Center of Zhejiang University (Hangzhou, China). All experiments were performed in compliance with the Guide for the Care and Use of Laboratory Animals published by the National Institutes of Health (Bethesda, MD, USA) and approved by the Ethics Committee on Animal Experimentation of Zhejiang University.

### 2.2 Animal grouping

Rats were randomly divided into following four groups ($n$=8): (1) control group, rat hearts were not preserved in Celsior solution; (2) Celsior group, rat hearts were preserved in Celsior solution for 12 h at 4 °C; (3) RGFP966 group, rat hearts were preserved in Celsior solution containing RGFP966 (at 0.25, 0.50, or 0.75 μmol/L; Selleck Chemicals, Houston, TX, USA) for 12 h at 4 °C; (4) RGFP966+verteporfin (VP) group, rat hearts were preserved in Celsior solution containing 0.75 μmol/L RGFP966 and 10 μg/mL VP

(Selleck Chemicals, Houston, TX, USA) for 12 h at 4 °C. After that, all hearts in the above groups were perfused with Krebs-Henseleit solution for 60 min.

Components of the Celsior solution (pH 7.4) included: NaOH 100 mmol/L, KCl 15 mmol/L, $MgCl_2$ 13 mmol/L, $CaCl_2$ 0.25 mmol/L, mannitol 60 mmol/L, lactobionate 80 mmol/L, histidine 30 mmol/L, and glutamate 20 mmol/L. Components of the Krebs-Henseleit solution (pH 7.4) included: NaCl 118 mmol/L, $NaHCO_3$ 3.25 mmol/L, $KH_2PO_4$ 1.2 mmol/L, $MgSO_4$ 1.2 mmol/L, KCl 4.7 mmol/L, and glucose 10 mmol/L. The Krebs-Henseleit solution was saturated with 95% $O_2$ and 5% $CO_2$.

### 2.3 Perfusion of isolated rat hearts

Isolated rat hearts were hypothermically preserved and reperfused as previously reported (Chen et al., 2016). Briefly, after the rats were anesthetized intraperitoneally with 1% (0.01 g/mL) sodium pentobarbital (50 mg/kg), their hearts were quickly removed and fixed on a Langendorff perfusion device. Then they were perfused with Krebs-Henseleit solution at 37 °C and a constant pressure of 76 mmHg. After 30 min of balanced perfusion, the hearts were transferred into Celsior solution (4 °C) to stop heart palpitations. Then the hearts were preserved in Celsior solution for 12 h with or without RGFP966/VP, followed by 60 min of reperfusion.

### 2.4 Measurement of cardiac function

A balloon sensor was inserted into left ventricle through the left atrial appendage of each perfused isolated heart. Cardiac functions were measured using a MedLab Biological Signal Acquisition and Processing System (Nanjing, China). The parameters included left ventricular end-diastolic pressure (LVEDP), left ventricular developed pressure (LVDP), maximal systolic and diastolic velocity of left ventricular pressure ($\pm dP/dt_{max}$), heart rate (HR), and coronary flow.

### 2.5 Western blotting

Total cellular protein was extracted by lysing left ventricle apical tissue using radioimmunoprecipitation assay (RIPA) buffer containing phenylmethanesulfonyl fluoride (Beyotime Institute of Biotechnology, Shanghai, China). Nuclear protein was obtained using a Cytoplasmic and Nuclear Extraction kit (Invent Biotechnologies, Plymouth, MN, USA). The equivalent protein (20 μg) was loaded on a 10% (0.1 g/mL) sodium dodecyl sulfate polyacrylamide gel electrophoresis (SDS-PAGE) gel. After electrophoresis (Bio-Rad, Hercules, CA, USA), proteins were transferred to a nitrocellulose membrane. The membrane was blocked with 5% (0.05 g/mL) skimmed milk for 1 h and incubated with primary antibodies overnight at 4 °C. The primary antibodies (Cell Signaling Technology, Danvers, MA, USA) were as follows: anti-HDAC3 (1:1000 diluted; Cat. No. 85057), anti-phosphorylated mammalian STE20-like kinase-1 (p-Mst1) (1:1000; Cat. No. 49332), anti-Mst1 (1:1000; Cat. No. 14946), anti-p-YAP (Ser127) (1:1000; Cat. No. 13008), anti-YAP (1:1000; Cat. No. 14074), anti-cleaved caspase-3 (1:1000; Cat. No. 9661), anti-B-cell lymphoma protein 2 (Bcl-2) (1:1000; Cat. No. 3498), anti-Bcl-2 associated X (Bax) (1:1000; Cat. No. 14796), anti-Histone H3 (1:1000; Cat. No. 4499), and anti-β-actin (1:1000; Cat. No. 3700). The membrane was then incubated with near-infrared-labeled secondary antibodies (1:5000, Li-COR Biosciences, Lincoln, NE, USA) at room temperature for 1 h. Strips were detected using an Odyssey CLx near infrared dual-color fluorescence imaging system (Li-COR Biosciences, Lincoln, NE, USA) and quantified using Image Studio Ver. 5.2 software.

### 2.6 Real-time quantitative polymerase chain reaction

Left ventricular myocardium tissue was homogenized in RNAiso Plus buffer (TaKaRa Bio, Inc., Mountain View, CA, USA) containing chloroform. Total RNA was precipitated and purified with isopropanol and ethanol, and then reverse-transcribed into complementary DNA (cDNA) using PrimeScript™ RT Master Mix (Perfect Real Time) (TaKaRa Bio, Inc.). Polymerase chain reaction (PCR) reaction solution including 10 μL 2× TB Green Premix Ex Taq II, 0.8 μL PCR forward primer (10 μmol/L), 0.8 μL PCR reverse primer (10 μmol/L), 0.4 μL 50× ROX Reference Dye, 2 μL cDNA, and 6 μL diethyl pyrocarbonate (DEPC) water was prepared in an ice bath. PCR amplification was performed using an ABI 7500 Fast Real-Time PCR system (Life Technologies, Austin, TX, USA). Primer sequences were as follows (forward and reverse, respectively): *SOD*, 5'-GGCC AAGGGAGATGTTACAA-3' and 5'-GAACCTTGGA

CTCCCACAGA-3'; *GPx*, 5'-CGGTTTCCCGTGCAATCAGT-3' and 5'-ACACCGGGGACCAAATGATG-3'; *CAT*, 5'-CCTGACATGGTCTGGGACTT-3' and 5'-CAAGTTTTTGATGCCCTGGT-3'; *Bcl-2*, 5'-ATGTGTGTGGAGAGCGTCAACC-3' and 5'-CCAGGAGAAATCAAACAGAGGC-3'; *GAPDH*, 5'-GACATCAAGAAGGTGGTG-3' and 5'-CAGCATCAAAGGTGGAAG-3'. The relative expression of genes was calculated by the $2^{-\Delta\Delta C_T}$ method (Lerman et al., 2018).

### 2.7 Determination of LDH activity

Lactate dehydrogenase (LDH) activity of coronary flow was determined using an LDH determination kit according to the manufacturer's protocol (Nanjing Jiancheng Institute of Bioengineering, Nanjing, China). Optical density was measured at 440 nm by a microplate reader (Thermo scientific, Waltham, MA, USA).

### 2.8 Detection of SOD activity, CAT activity, MDA content, and GPx activity

Left ventricular myocardium tissue was homogenized in lysis buffer (Beyotime Institute of Biotechnology, Shanghai, China). The supernatant was collected after centrifugation at 12000 r/min, at 4 °C for 10 min. The SOD activity, CAT activity, malondialdehyde (MDA) content, and glutathione peroxidase (GPx) activity were determined using SOD activity test kit (Beyotime Institute of Biotechnology), CAT determination kit (Nanjing Jiancheng Institute of Bioengineering), MDA test kit (Beyotime Institute of Biotechnology), and GPx detection kit (Beyotime Institute of Biotechnology), respectively. Optical densities were measured at 450, 405, 532, and 340 nm, respectively, by a microplate reader (Thermo scientific).

### 2.9 Immunohistochemistry

Left ventricular tissue was fixed in 10% neutral formalin solution, and then embedded in paraffin. After being dewaxed and dehydrated, 4-μm thick tissue slices were dyed with hematoxylin and eosin. The slices were observed under an optical microscope (Olympus, Japan).

### 2.10 Detection of apoptosis using TUNEL method

Apoptotic cells were detected using an In Situ Cell Death Detection kit (Roche Diagnostics GmbH, Mannheim, Germany). Briefly, after being dewaxed and hydrated, slices of left ventricular tissue were soaked in permeabilisation solution (containing 0.1% Triton X-100 and 0.1% sodium citrate solution) for 10 min. Then slices were incubated with terminal deoxynucleotidyl-transferase (TdT)-mediated dUTP nick-end labeling (TUNEL) reaction solution at 37 °C for 1 h in darkness. After being thoroughly washed, specimens were incubated with converter-peroxidase (POD) at 37 °C for 30 min in darkness and dyed with diaminobenzidine (DAB) and hematoxylin. The number of apoptotic cells (brown) was calculated from observations under an optical microscope (Olympus, Japan) (Chen et al., 2018).

### 2.11 Statistical analysis

Data are expressed as mean±standard error of mean (SEM). Differences between groups were analyzed by one-way analysis of variance (ANOVA) with Tukey's multiple comparisons test using Prism 8.0.1 (GraphPad Software, Inc., La Jolla, CA, USA).

## 3 Results

### 3.1 Inhibition of HDAC3 protein expression by RGFP966 in rat hearts subjected to hypothermic preservation

Hypothermic preservation significantly increased HDAC3 protein expression in rat hearts. The HDAC3 inhibitor RGFP966 inhibited the increase of hypothermic preservation-induced HDAC3 protein expression in a concentration-dependent manner ($P<0.01$; Fig. 1).

### 3.2 Recovery of cardiac function promoted by RGFP966 in hypothermically preserved rat hearts

At the end of balanced perfusion, cardiac functions among the different groups were similar ($P>0.05$, data not shown). At the end of 60 min of reperfusion after hypothermic preservation, LVEDP was higher than that of the control group, while LVDP, $\pm dP/dt_{max}$, HR, and coronary flow were lower than those of the control group ($P<0.01$; Fig. 2). These hypothermic preservation-induced injuries were significantly alleviated by supplementation with RGFP966 ($P<0.05$; Fig. 2). RGFP966 (0.75 μmol/L) was chosen to further explore the mechanism of RGFP966-induced cardioprotection.

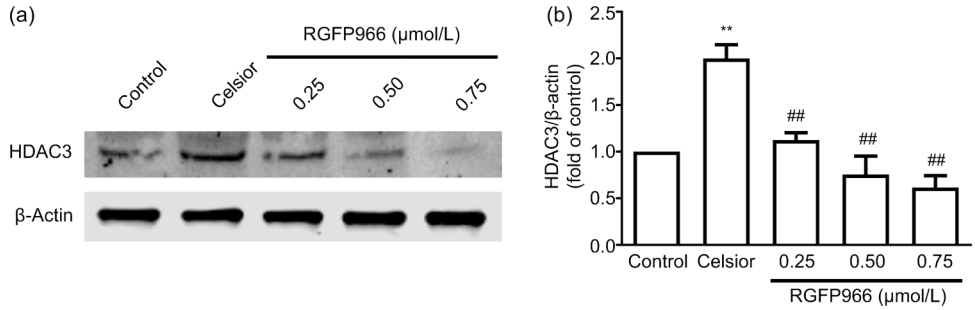


**Fig. 1 Effect of RGFP966 on HDAC3 expression in hypothermically preserved rat hearts**

(a) Representative immunoblot obtained with histone deacetylase 3 (HDAC3) and β-actin antibodies. (b) Densitometric analysis showing the expression of HDAC3. β-Actin served as an internal control. Data are shown as mean±standard error of mean (SEM) of four independent experiments, expressed as a fold increase relative to the value of the control group. $^{**}$ $P$<0.01 vs. control group; $^{\#\#}$ $P$<0.01 vs. Celsior group

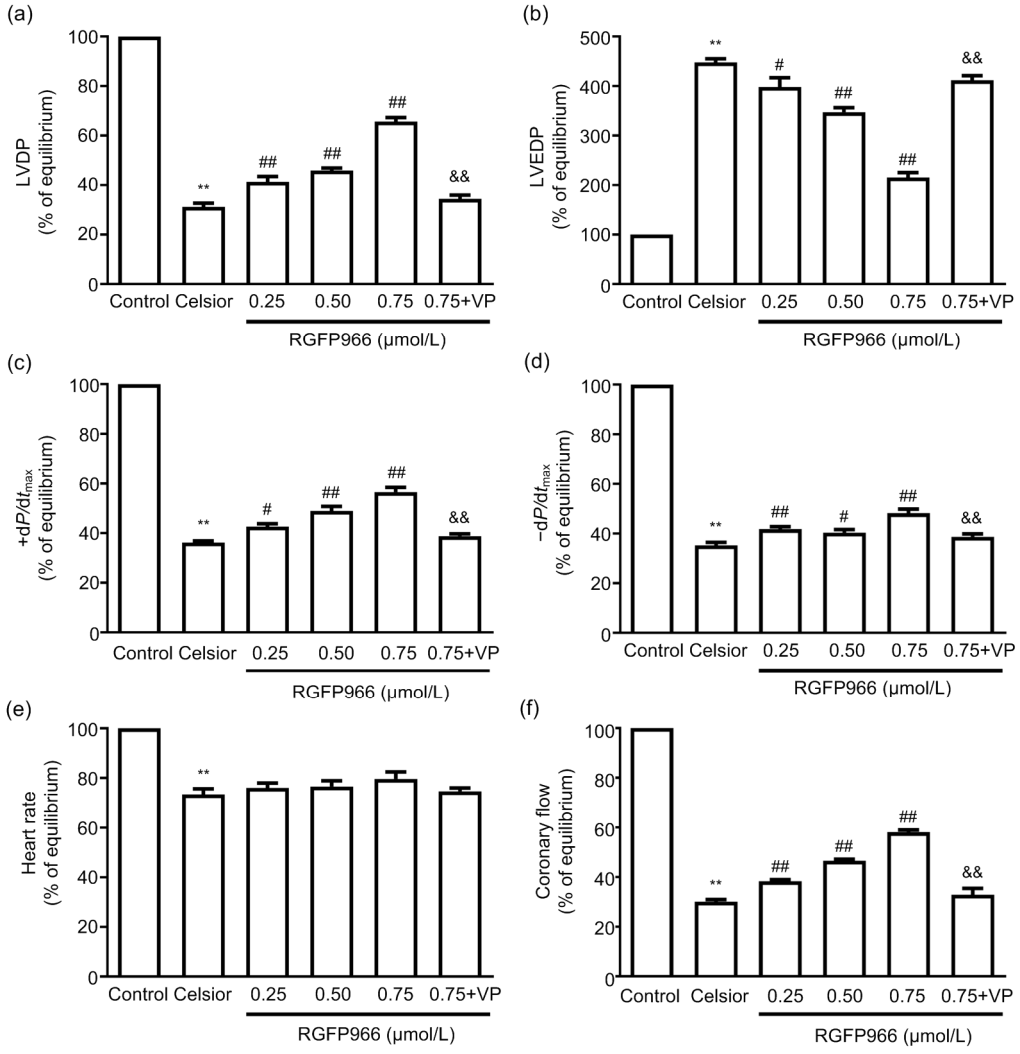


**Fig. 2 Hemodynamic parameters after 60 min of reperfusion following hypothermic preservation**

(a) Left ventricular developed pressure (LVDP); (b) Left ventricular end-diastolic pressure (LVEDP); (c) Maximal systolic velocity of left ventricular pressure (+d$P$/d$t_{max}$); (d) Maximal diastolic velocity of left ventricular pressure (−d$P$/d$t_{max}$); (e) Heart rate; (f) Coronary flow. Data are shown as mean±standard error of mean (SEM) ($n$=8). $^{**}$ $P$<0.01 vs. control group; $^{\#}$ $P$<0.05, $^{\#\#}$ $P$<0.01 vs. Celsior group; $^{\&\&}$ $P$<0.01 vs. RGFP966 (0.75 μmol/L) group. VP: verteporfin

### 3.3 Inhibition of the hypothermic preservation-induced activation of Hippo-YAP signaling pathway by RGFP966

After hypothermic preservation, total Mst1 protein expression did not change, but the p-Mst1/Mst1 ratio increased significantly ($P$<0.01; Figs. 3a and 3b). Hypothermic preservation also decreased total YAP protein expression and increased the p-YAP/YAP ratio ($P$<0.01; Figs. 3a, 3d, and 3e). Compared with the Celsior group, RGFP966 (0.75 μmol/L) significantly inhibited the increase of the p-Mst1/Mst1 and p-YAP/YAP ratios induced by hypothermic preservation, and prevented a reduction in total YAP protein expression ($P$<0.01; Fig. 3).

### 3.4 Abolishment of RGFP966-induced improvement of cardiac function by VP

Hypothermic preservation reduced the nuclear YAP protein level; however, this was prevented by RGFP966 ($P$<0.01; Figs. 4a and 4b). VP, a small molecular inhibitor of YAP–TEAD interaction, partially abolished the protective effect of RGFP966 on cardiac function ($P$<0.01; Fig. 2). RGFP966 also prevented hypothermic preservation-induced increases of LDH activity and MDA content. This was also reversed by VP ($P$<0.01; Figs. 4c and 4d).

### 3.5 Inhibition of hypothermic preservation-induced oxidative stress by RGFP966

Hypothermic preservation reduced the expression of antioxidant genes (*SOD*, *GPx*, and *CAT*) and inhibited SOD, GPx, and CAT activity. Compared with the Celsior group, RGFP966 significantly increased *SOD*, *GPx*, and *CAT* mRNA expression and enhanced their activity. The beneficial effects of RGFP966 were cancelled by addition of VP ($P$<0.05; Figs. 5a−5c, Fig. 6).

### 3.6 Inhibition of hypothermic preservation-induced apoptosis by RGFP966

After hypothermic preservation, the arrangement of myocardial fibers was disordered and the gaps between them widened (Fig. 7a). The number of apoptotic cells also increased ($P$<0.01; Figs. 7b and 7c). RGFP966 improved myocardial morphology and reduced the number of apoptotic cells. The above effect was prevented by supplementation with VP (Fig. 7).

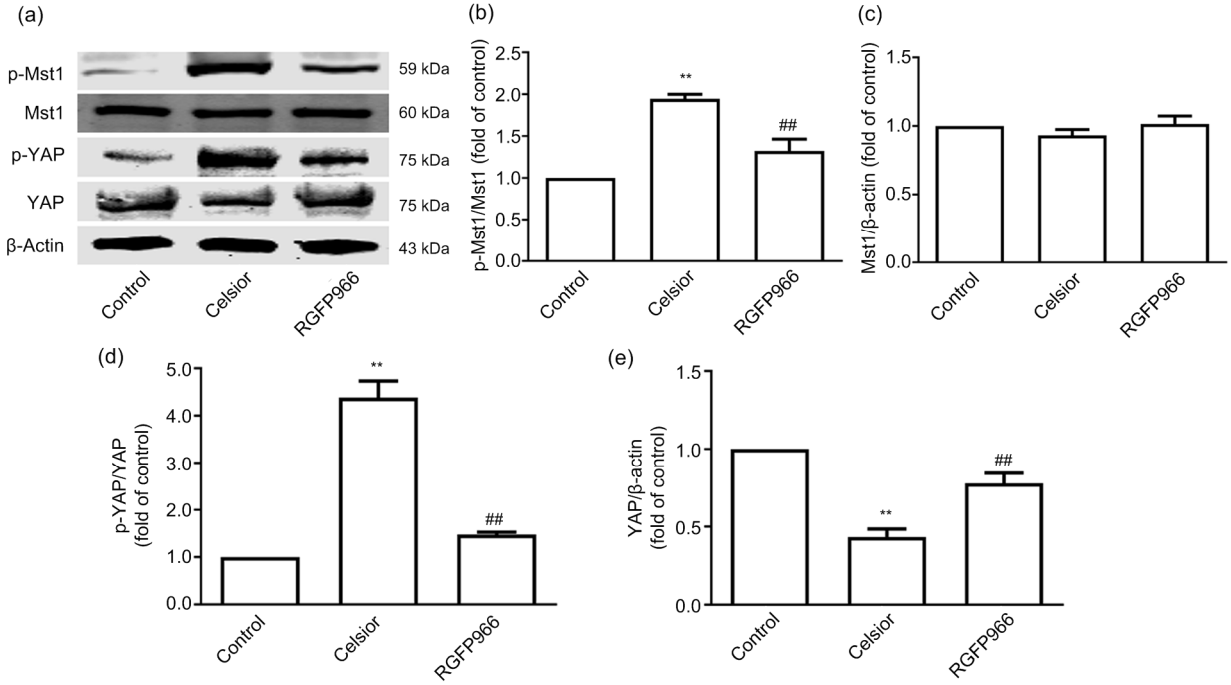


**Fig. 3 Inhibition of the hypothermic preservation-induced activation of Hippo-YAP signaling pathway by RGFP966**
(a) Representative immunoblot obtained with phosphorylated mammalian STE20-like kinase-1 (p-Mst1), Mst1, p-Yes-associated protein (YAP), YAP, and β-actin antibodies. (b–e) Densitometric analysis showing the expression of p-Mst1/Mst1 (b), total Mst1 (c), p-YAP/YAP (d), and total YAP (e). β-Actin served as an internal control. Data are shown as mean±standard error mean (SEM) of three independent experiments, expressed as a fold increase relative to the value of the control group. ** $P$<0.01 vs. control group; ## $P$<0.01 vs. Celsior group

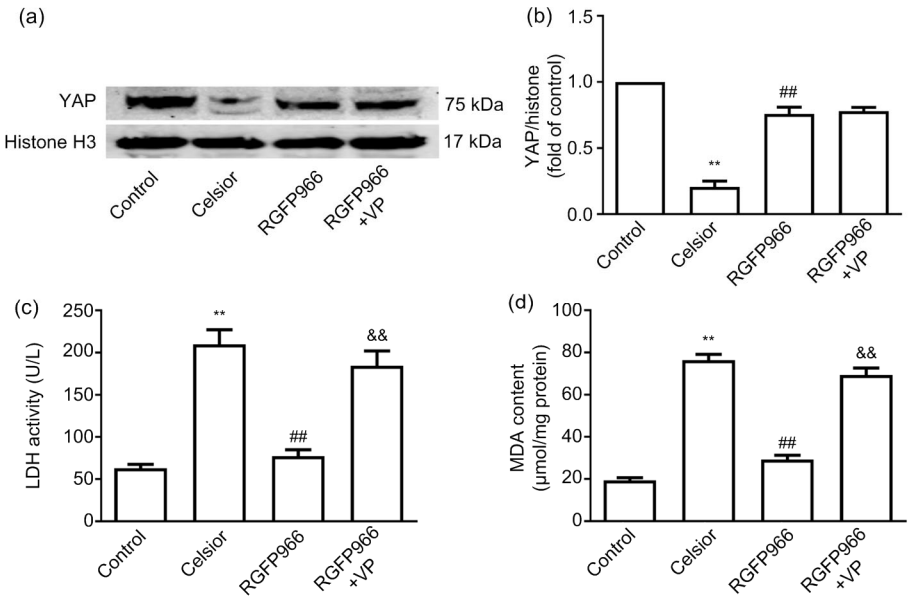


**Fig. 4 Effects of RGFP966 on nuclear YAP protein, LDH activity, and MDA content in rat hearts subjected to 12 h of hypothermic preservation**

(a) Representative immunoblot obtained with Yes-associated protein (YAP) and histone H3 antibodies. (b) Densitometric analysis showing the expression of nuclear YAP. Histone H3 served as a nuclear internal control. Data are mean±standard error of mean (SEM) of four independent experiments, expressed as a fold increase relative to the value of the control group. (c, d) Lactate dehydrogenase (LDH) activity and malondialdehyde (MDA) content. Data are shown as mean±SEM ($n$=8). $^{**}$ $P$<0.01 vs. control group; $^{\#\#}$ $P$<0.01 vs. Celsior group; $^{\&\&}$ $P$<0.01 vs. RGFP966 group. VP: verteporfin

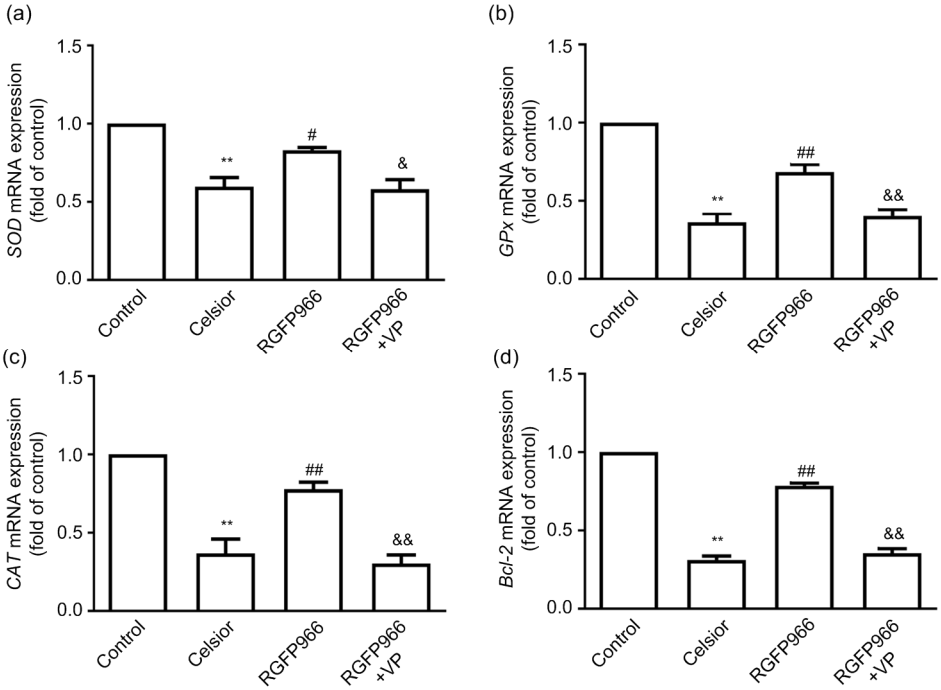


**Fig. 5 Effects of RGFP966 on *SOD*, *GPx*, *CAT*, and *Bcl-2* expression in rat hearts subjected to 12 h of hypothermic preservation**

(a) Expression of superoxide dismutase (*SOD*); (b) Expression of glutathione peroxidase (*GPx*); (c) Expression of catalase (*CAT*); (d) Expression of B-cell lymphoma protein 2 (*Bcl-2*). Data are shown as mean±standard error of mean (SEM) ($n$=3). $^{**}$ $P$<0.01 vs. control group; $^{\#}$ $P$<0.05, $^{\#\#}$ $P$<0.01 vs. Celsior group; $^{\&}$ $P$<0.05, $^{\&\&}$ $P$<0.01 vs. RGFP966 group. VP: verteporfin

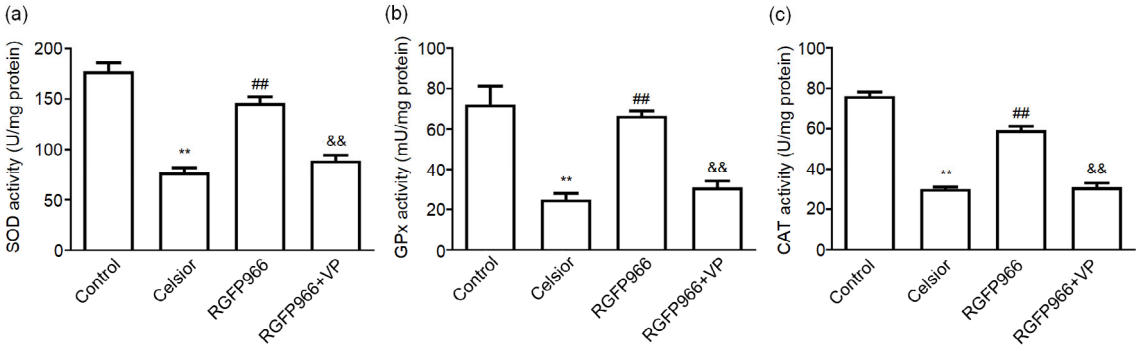


**Fig. 6 Effects of RGFP966 on SOD, GPx, and CAT activity in rat hearts subjected to 12 h of hypothermic preservation**
(a) Activity of superoxide dismutase (SOD); (b) Activity of glutathione peroxidase (GPx); (c) Activity of catalase (CAT). Data are shown as mean±standard error of mean (SEM) ($n$=8). $^{**}$ $P$<0.01 vs. control group; $^{\#\#}$ $P$<0.01 vs. Celsior group; $^{\&\&}$ $P$<0.01 vs. RGFP966 group. VP: verteporfin

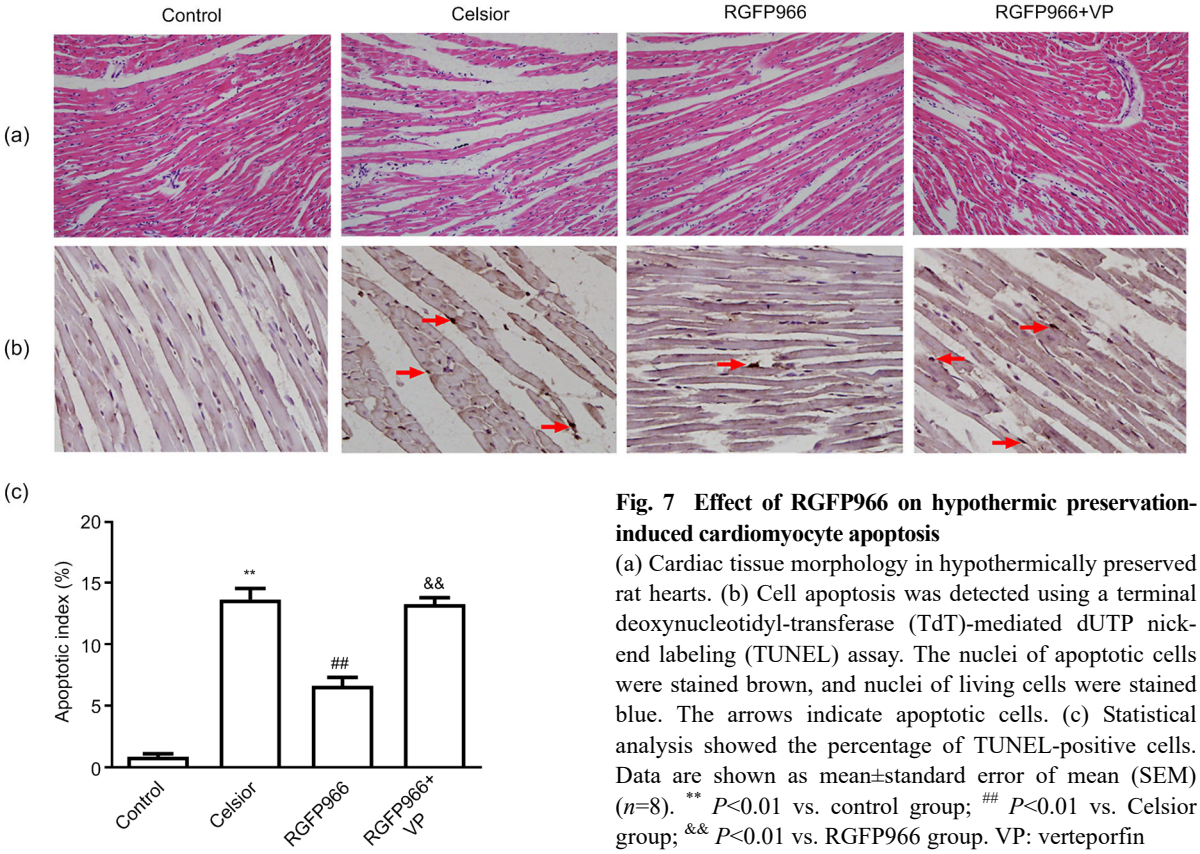


**Fig. 7 Effect of RGFP966 on hypothermic preservation-induced cardiomyocyte apoptosis**
(a) Cardiac tissue morphology in hypothermically preserved rat hearts. (b) Cell apoptosis was detected using a terminal deoxynucleotidyl-transferase (TdT)-mediated dUTP nick-end labeling (TUNEL) assay. The nuclei of apoptotic cells were stained brown, and nuclei of living cells were stained blue. The arrows indicate apoptotic cells. (c) Statistical analysis showed the percentage of TUNEL-positive cells. Data are shown as mean±standard error of mean (SEM) ($n$=8). $^{**}$ $P$<0.01 vs. control group; $^{\#\#}$ $P$<0.01 vs. Celsior group; $^{\&\&}$ $P$<0.01 vs. RGFP966 group. VP: verteporfin

RGFP966 inhibited hypothermic preservation-induced overexpression of Bax and cleaved caspase-3, and enhanced Bcl-2 mRNA and protein expression ($P$<0.01; Figs. 8 and 5d). Compared with the RGFP966 group, Bax and cleaved caspase-3 protein were higher, and Bcl-2 mRNA and protein were lower in the RGFP966+VP group ($P$<0.01; Figs. 8 and 5d).

## 4 Discussion

Both in vitro and in vivo studies indicate that overexpression of HDAC3 is involved in cardiac ischemia-reperfusion injury, development of hypertension, heart failure, and atrial fibrillation, while inhibition of HDAC3 alleviates cardiac injury and

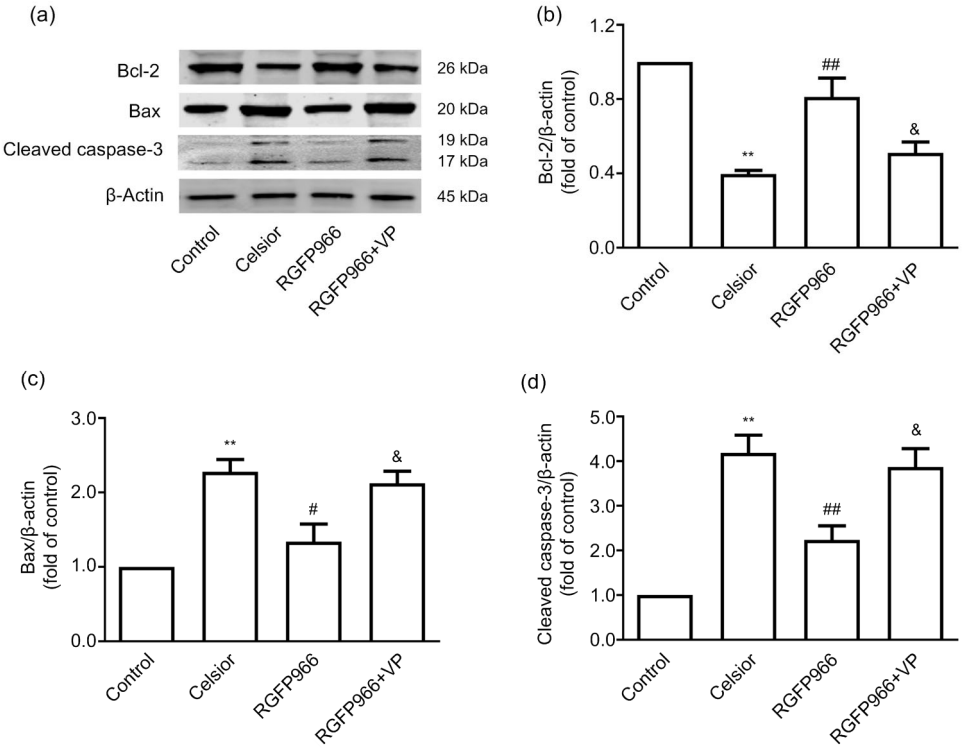


**Fig. 8 Effects of RGFP966 on proapoptotic and antiapoptotic protein expression in rat isolated hearts subjected to hypothermic preservation**

(a) Representative immunoblot obtained with B-cell lymphoma protein 2 (Bcl-2), Bcl-2-associated X (Bax), cleaved caspase-3, and β-actin antibodies. (b–d) Densitometric analysis showing the expression of Bcl-2 (b), Bax (c), and cleaved caspase-3 (d). β-Actin served as an internal control. Data are shown as mean±standard error of mean (SEM) of four independent experiments, expressed as a fold increase relative to the value of the control group. $^{**}$ $P$<0.01 vs. control group; $^{\#}$ $P$<0.05, $^{\#\#}$ $P$<0.01 vs. Celsior group; $^{\&}$ $P$<0.05 vs. RGFP966 group. VP: verteporfin

cardiac remodeling (Sharifi-Sanjani et al., 2014; Chen et al., 2017; Zhang DL et al., 2018; Ryu et al., 2019). Moreover, it has been proved that RGFP966 can alleviate cerebral ischemia-reperfusion injury by reducing HDAC3 protein expression in diabetic mice (Zhao et al., 2019). In the present study, we confirmed that the HDAC3 protein was overexpressed in rat hearts subjected to 12 h of hypothermic preservation, while downregulation of HDAC3 by RGFP966 could prevent hypothermic preservation-induced cardiac dysfunction and promote cardiac function recovery during reperfusion. LVDP and $+\mathrm{d}P/\mathrm{d}t_{\max}$ were used to evaluate the cardiac systolic function, while LVEDP and $-\mathrm{d}P/\mathrm{d}t_{\max}$ were used to indicate the cardiac diastolic function. It has been reported that $\mathrm{d}P/\mathrm{d}t_{\max}$ is determined not only by ventricular contractility, but also by preload and afterload (Hamlin and del Rio, 2012). In the Langendorff perfusion system, an isolated rat heart is perfused at a fixed perfusion pressure (afterload). The balloon containing a known volume of fluid inserted into the left ventricle also allows cardiac contraction independent of ventricular preload (end-diastolic volume). So, in this study, the preload and afterload were held constant, and the $\mathrm{d}P/\mathrm{d}t_{\max}$ was considered mainly as a sensitive indicator of myocardial contractility. The coronary flow, which is associated with coronary artery diameter at a constant perfusion pressure, indicates the extent of coronary dilation or myocardial blood supply. Recent studies have shown that the beneficial effect of HDAC inhibitors is dependent on Hippo signaling (Jung et al., 2017; Rivera-Reyes et al., 2018; Yu et al., 2018). The Hippo pathway is a kinase cascade reaction, in which the p-Mst1/2 (ortholog of Drosophila Hippo) activates long acting thyroid stimulator 1/2 (LATS1/2) kinases, and in turn phosphorylates YAP/TAZ. The p-YAP/TAZ is then sequestered in the cytoplasm and degraded via ubiquitination. When

dephosphorylated, YAP/TAZ is translocated into nucleus and induces TEADs-mediated gene transcription, inhibits apoptosis, and promotes cell survival (Jung et al., 2017). Inhibition of HDAC3 attenuated oxidative stress, decreased neuronal apoptosis in the hippocampi, and improved the spatial memory function of Alzheimer's disease model mice by reducing p-Mst1 and p-YAP expression levels (Yu et al., 2018). HDAC inhibitor could also inhibit mammalian target of rapamycin (mTOR) signaling, upregulate protein kinase R (PKR)-like endoplasmatic reticulum kinase (PERK) and ataxia telangiectasia mutated (ATM)- and RAD3-related kinases 6 (ATR6)-mediated unfolded protein response, and increase autophagy via downregulation of YAP protein (Rivera-Reyes et al., 2018). Our present study showed that hypothermic preservation increased phosphorylation of Mst1 and YAP. RGFP966 suppressed phosphorylation of YAP, stabilized total YAP expression, and increased nuclear localization of YAP. VP, an inhibitor of YAP–TEAD interaction, prevented RGFP966-induced improvement of cardiac function in hypothermically preserved rat hearts, suggesting that the Hippo-YAP signaling pathway was involved in the beneficial effect of RGFP966 on rat hearts subjected to hypothermic preservation.

The Hippo-YAP signaling pathway plays an important role in cardiac physiological and pathophysiological conditions (Wang et al., 2018). Hippo-YAP signaling acts as a "signal integrator" in the regulation of oxidative stress and apoptosis. This is because YAP–TEAD interaction can lead to a higher expression of anti-apoptotic, antioxidant, and mitochondrial biogenesis genes that are critical for regulation of various cellular events (Roy et al., 2016; Zhang et al., 2016; Wang et al., 2018). SOD and glutathione gene expression was upregulated by YAP in riboflavinogenic fungus *Ashbya gossypii* (Kavitha and Chandra, 2014). Restoration of YAP activity upregulated the expression of the antioxidant genes *CAT* and *SOD*, and alleviated cardiac ischemia-reperfusion injury through a forkhead box O1 (FoxO1)-mediated mechanism (Shao et al., 2014). The Hippo-YAP signaling pathway is also involved in myocardial reperfusion injury associated with the dissociation of Bcl-xL from Bax, thereby promoting apoptosis (Nakamura et al., 2016). Overexpression of YAP reduced Bak and Bid expression, inhibited caspase-3 activation, decreased apoptosis, and delayed senescence of human periodontal ligament stem cells (Jia et al., 2018). Our present study showed that RGFP966 attenuated oxidative stress and increased expression of the antioxidant enzymes SOD, CAT, and GPx. RGFP966 also increased Bcl-2 expression, and inhibited caspase-3 activity and apoptosis. Inhibition of YAP and TEAD interaction abolished these RGFP966-induced antioxidant and anti-apoptosis effects. The results suggest that the Hippo-YAP pathway participates in RGFP966-induced cardiac protection via regulation of oxidative stress and apoptosis. However, VP did not fully abolish the protective effect of RGFP966, suggesting that other signaling pathways beyond YAP might also be involved.

Some studies demonstrated that the beneficial effect of RGFP966 could be accounted for by an epigenetic modulation mechanism (Xu et al., 2017; Hitchcock et al., 2019). However, other studies reported that HDAC3 regulates embryonic development and lipid metabolism in a deacetylase-independent manner (Sun et al., 2013; Lewandowski et al., 2015). HDAC inhibitor could also protect neurons from exogenous oxidative stress via an HDAC-independent mechanism (Olson et al., 2015). In rat cortical and spinal astrocytes, RGFP966 has been reported to exhibit its anti-inflammatory property through both HDAC3-dependent and HDAC3-independent mechanisms (Morioka et al., 2016). Whether RGFP966 regulates the YAP pathway in an HDAC3-dependent or HDAC3-independent manner is worthy of further investigation.

Therefore, supplementation of Celsior solution with RGFP966 can attenuate cardiac dysfunction induced by prolonged hypothermic preservation. The protective effect of RGFP966 on hypothermic preservation-induced myocardial injury may provide a valuable and feasible strategy for heart transplantation in clinical practice, making it possible for patients to obtain donor hearts from more distant locations, thereby expanding possible donor heart resources in the future.

There were some limitations in this study. Firstly, both YAP and TAZ are downstream signaling molecules in the Hippo pathway. It has been reported that YAP has a stronger effect on regulation of cellular function than TAZ (Plouffe et al., 2018). So, in the present study, we explored only the role of YAP in the

effect of RGFP966. The role of TAZ needs to be further investigated. Secondly, LDH, troponin, and creatine kinase-MB (CKMB) are three classic markers of myocardial injury. Only LDH was determined in the present study. Lack of evaluations of troponin and CKMB is a critical limitation. Finally, although the protective effect of RGFP966 on hypothermic preservation-induced myocardial injury has been demonstrated, further confirmation is needed before RGFP966 can be used in heart transplantation in clinical practice.

## 5 Conclusions

The results suggest that supplementation of Celsior solution with RGFP966 attenuated cardiac dysfunction induced by prolonged hypothermic preservation in rat hearts. The mechanism may involve inhibition of oxidative stress and apoptosis via inactivation of the YAP pathway.

### Contributors

Xiao-he ZHENG, Lin-lin WANG, Ming-zhi ZHENG, and Jin-jie ZHONG performed the experimental research and data analysis, wrote and edited the manuscript. Ying-ying CHEN and Yue-liang SHEN contributed to the study design, data analysis, writing and editing of the manuscript. All authors have read and approved the final manuscript and, therefore, have full access to all the data in the study and take responsibility for the integrity and security of the data.

### Compliance with ethics guidelines

Xiao-he ZHENG, Lin-lin WANG, Ming-zhi ZHENG, Jin-jie ZHONG, Ying-ying CHEN, and Yue-liang SHEN declare that they have no conflict of interest.

The research was conducted in accordance with the Declaration of Helsinki and/or with the Guide for the Care and Use of Laboratory Animals as adopted and promulgated by the United States National Institutes of Health. All experiments were approved by the Ethics Committee on Animal Experimentation of Zhejiang University (Hangzhou, China).

### References

An PP, Li JX, Lu LL, et al., 2019. Histone deacetylase 8 triggers the migration of triple negative breast cancer cells via regulation of YAP signals. *Eur J Pharmacol*, 845:16-23. https://doi.org/10.1016/j.ejphar.2018.12.030

Aune SE, Herr DJ, Mani SK, et al., 2014. Selective inhibition of class I but not class IIb histone deacetylases exerts cardiac protection from ischemia reperfusion. *J Mol Cell Cardiol*, 72:138-145. https://doi.org/10.1016/j.yjmcc.2014.03.005

Brundel BJJM, Li J, Zhang DL, 2020. Role of HDACs in cardiac electropathology: therapeutic implications for atrial fibrillation. *Biochim Biophys Acta Mol Cell Res*, 1867(3):118459. https://doi.org/10.1016/j.bbamcr.2019.03.006

Chen BY, Jiang LX, Hao K, et al., 2018. Protection of plasma transfusion against lipopolysaccharide/D-galactosamine-induced fulminant hepatic failure through inhibiting apoptosis of hepatic cells in mice. *J Zhejiang Univ-Sci B (Biomed & Biotechnol)*, 19(6):436-444. https://doi.org/10.1631/jzus.B1700277

Chen GG, Yan JB, Wang XM, et al., 2016. Mechanism of uncoupling protein 2-mediated myocardial injury in hypothermic preserved rat hearts. *Mol Med Rep*, 14(2):1857-1864. https://doi.org/10.3892/mmr.2016.5436

Chen ML, Liu Q, Chen LJ, et al., 2017. Remifentanil postconditioning ameliorates histone H3 acetylation modification in H9c2 cardiomyoblasts after hypoxia/reoxygenation via attenuating endoplasmic reticulum stress. *Apoptosis*, 22(5):662-671. https://doi.org/10.1007/s10495-017-1347-5

Ferguson BS, McKinsey TA, 2015. Non-sirtuin histone deacetylases in the control of cardiac aging. *J Mol Cell Cardiol*, 83:14-20. https://doi.org/10.1016/j.yjmcc.2015.03.010

Fu PF, Zheng X, Fan X, et al., 2019. Role of cytoplasmic lncRNAs in regulating cancer signaling pathways. *J Zhejiang Univ-Sci B (Biomed & Biotechnol)*, 20(1):1-8. https://doi.org/10.1631/jzus.B1800254

Hamlin RL, del Rio C, 2012. $dP/dt_{max}$—a measure of 'baroinometry'. *J Pharmacol Toxicol Methods*, 66(2):63-65. https://doi.org/10.1016/j.vascn.2012.01.001

Hitchcock LN, Raybuck JD, Wood MA, et al., 2019. Effects of a histone deacetylase 3 inhibitor on extinction and reinstatement of cocaine self-administration in rats. *Psychopharmacology*, 236(1):517-529. https://doi.org/10.1007/s00213-018-5122-2

Janczura KJ, Volmar CH, Sartor GC, et al., 2018. Inhibition of HDAC3 reverses Alzheimer's disease-related pathologies in vitro and in the 3xTg-AD mouse model. *Proc Natl Acad Sci USA*, 115(47):E11148-E11157. https://doi.org/10.1073/pnas.1805436115

Jia LL, Gu WT, Zhang YP, et al., 2018. Activated Yes-associated protein accelerates cell cycle, inhibits apoptosis, and delays senescence in human periodontal ligament stem cells. *Int J Med Sci*, 15(11):1241-1250. https://doi.org/10.7150/ijms.25115

Joshi AD, Barabutis N, Birmpas C, et al., 2015. Histone deacetylase inhibitors prevent pulmonary endothelial hyperpermeability and acute lung injury by regulating heat shock protein 90 function. *Am J Physiol Lung Cell Mol Physiol*, 309(12):L1410-L1419. https://doi.org/10.1152/ajplung.00180.2015

Jung DE, Park SB, Kim K, et al., 2017. CG200745, an HDAC

inhibitor, induces anti-tumour effects in cholangiocarcinoma cell lines via miRNAs targeting the Hippo pathway. *Sci Rep*, 7:10921. https://doi.org/10.1038/s41598-017-11094-3

Kavitha S, Chandra TS, 2014. Oxidative stress protection and glutathione metabolism in response to hydrogen peroxide and menadione in riboflavinogenic fungus *Ashbya gossypii*. *Appl Biochem Biotechnol*, 174(6):2307-2325. https://doi.org/10.1007/s12010-014-1188-4

Korkmaz-Icöz S, Li SL, Huttner R, et al., 2019. Hypothermic perfusion of donor heart with a preservation solution supplemented by mesenchymal stem cells. *J Heart Lung Transplant*, 38(3):315-326. https://doi.org/10.1016/j.healun.2018.12.003

Lerman DA, Diaz M, Peault B, 2018. Changes in coexpression of pericytes and endogenous cardiac progenitor cells from heart development to disease state. *Eur Heart J*, 39(S1):P1850. https://doi.org/10.1093/eurheartj/ehy565.P1850

Lewandowski SL, Janardhan HP, Trivedi CM, 2015. Histone deacetylase 3 coordinates deacetylase-independent epigenetic silencing of transforming growth factor-β1 (TGF-β1) to orchestrate second heart field development. *J Biol Chem*, 290(45):27067-27089. https://doi.org/10.1074/jbc.M115.684753

Li H, Li XJ, Jing XZ, et al., 2018. Hypoxia promotes maintenance of the chondrogenic phenotype in rat growth plate chondrocytes through the HIF-1α/YAP signaling pathway. *Int J Mol Med*, 42(6):3181-3192. https://doi.org/10.3892/ijmm.2018.3921

Lkhagva B, Lin YK, Kao YH, et al., 2015. Novel histone deacetylase inhibitor modulates cardiac peroxisome proliferator-activated receptors and inflammatory cytokines in heart failure. *Pharmacology*, 96(3-4):184-191. https://doi.org/10.1159/000438864

Malvaez M, McQuown SC, Rogge GA, et al., 2013. HDAC3-selective inhibitor enhances extinction of cocaine-seeking behavior in a persistent manner. *Proc Natl Acad Sci USA*, 110(7):2647-2652. https://doi.org/10.1073/pnas.1213364110

McKinsey TA, 2012. Therapeutic potential for HDAC inhibitors in the heart. *Annu Rev Pharmacol Toxicol*, 52:303-319. https://doi.org/10.1146/annurev-pharmtox-010611-134712

Mehra MR, Canter CE, Hannan MM, et al., 2016. The 2016 international society for heart lung transplantation listing criteria for heart transplantation: a 10-year update. *J Heart Lung Transplant*, 35(1):1-23. https://doi.org/10.1016/j.healun.2015.10.023

Morioka N, Tomori M, Zhang FF, et al., 2016. Stimulation of nuclear receptor REV-ERBs regulates tumor necrosis factor-induced expression of proinflammatory molecules in C6 astroglial cells. *Biochem Biophys Res Commun*, 469(2):151-157. https://doi.org/10.1016/j.bbrc.2015.11.086

Nakamura M, Zhai PY, del Re DP, et al., 2016. Mst1-mediated phosphorylation of Bcl-xL is required for myocardial reperfusion injury. *JCI Insight*, 1(5):e86217. https://doi.org/10.1172/jci.insight.86217

Olson DE, Sleiman SF, Bourassa MW, et al., 2015. Hydroxamate-based histone deacetylase inhibitors can protect neurons from oxidative stress via a histone deacetylase-independent catalase-like mechanism. *Chem Biol*, 22(4):439-445. https://doi.org/10.1016/j.chembiol.2015.03.014

Plouffe SW, Lin KC, Moore JL 3rd, et al., 2018. The Hippo pathway effector proteins YAP and TAZ have both distinct and overlapping functions in the cell. *J Biol Chem*, 293(28):11230-11240. https://doi.org/10.1074/jbc.RA118.002715

Poleshko A, Shah PP, Gupta M, et al., 2017. Genome-nuclear lamina interactions regulate cardiac stem cell lineage restriction. *Cell*, 171(3):573-587.e14. https://doi.org/10.1016/j.cell.2017.09.018

Ren WB, Xia XJ, Huang J, et al., 2019. Interferon-γ regulates cell malignant growth via the c-Abl/HDAC2 signaling pathway in mammary epithelial cells. *J Zhejiang Univ-Sci B (Biomed & Biotechnol)*, 20(1):39-48. https://doi.org/10.1631/jzus.B1800211

Rivera-Reyes A, Ye S, Marino GE, et al., 2018. YAP1 enhances NF-κB-dependent and independent effects on clock-mediated unfolded protein responses and autophagy in sarcoma. *Cell Death Dis*, 9(11):1108. https://doi.org/10.1038/s41419-018-1142-4

Roy A, Lordier L, Pioche-Durieu C, et al., 2016. Uncoupling of the Hippo and Rho pathways allows megakaryocytes to escape the tetraploid checkpoint. *Haematologica*, 101(12):1469-1478. https://doi.org/10.3324/haematol.2016.149914

Ryu Y, Kee HJ, Sun SM, et al., 2019. Class I histone deacetylase inhibitor MS-275 attenuates vasoconstriction and inflammation in angiotensin II-induced hypertension. *PLoS ONE*, 14(3):e0213186. https://doi.org/10.1371/journal.pone.0213186

Schmitt HM, Schlamp CL, Nickells RW, 2018. Targeting HDAC3 activity with RGFP966 protects against retinal ganglion cell nuclear atrophy and apoptosis after optic nerve injury. *J Ocul Pharmacol Ther*, 34(3):260-273. https://doi.org/10.1089/jop.2017.0059

Shao D, Zhai PY, del Re DP, et al., 2014. A functional interaction between Hippo-YAP signalling and FoxO1 mediates the oxidative stress response. *Nat Commun*, 5(1):3315. https://doi.org/10.1038/ncomms4315

Sharifi-Sanjani M, Shoushtari AH, Quiroz M, et al., 2014. Cardiac CD47 drives left ventricular heart failure through $Ca^{2+}$-CaMKII-regulated induction of HDAC3. *J Am Heart Assoc*, 3(3):e000670. https://doi.org/10.1161/JAHA.113.000670

Sun Z, Feng D, Fang B, et al., 2013. Deacetylase-independent function of HDAC3 in transcription and metabolism requires nuclear receptor corepressor. *Mol Cell*, 52(6):769-782. https://doi.org/10.1016/j.molcel.2013.10.022

Wang J, Liu SJ, Heallen T, et al., 2018. The Hippo pathway in the heart: pivotal roles in development, disease, and regeneration. *Nat Rev Cardiol*, 15(11):672-684.

https://doi.org/10.1038/s41569-018-0063-3

Xu Z, Tong Q, Zhang ZG, et al., 2017. Inhibition of HDAC3 prevents diabetic cardiomyopathy in OVE26 mice via epigenetic regulation of DUSP5-ERK1/2 pathway. *Clin Sci (Lond)*, 131(15):1841-1857. https://doi.org/10.1042/CS20170064

Yu LJ, Liu Y, Jin YXZ, et al., 2018. Lentivirus-mediated HDAC3 inhibition attenuates oxidative stress in APPswe/PS1dE9 mice. *J Alzheimers Dis*, 61(4):1411-1424. https://doi.org/10.3233/JAD-170844

Zhang DL, Hu X, Li J, et al., 2018. Converse role of class I and class IIa HDACs in the progression of atrial fibrillation. *J Mol Cell Cardiol*, 125:39-49. https://doi.org/10.1016/j.yjmcc.2018.09.010

Zhang H, Geng DC, Gao J, et al., 2016. Expression and significance of Hippo/YAP signaling in glioma progression. *Tumor Biol*, 37(12):15665-15676. https://doi.org/10.1007/s13277-016-5318-1

Zhang J, Xu Z, Gu JL, et al., 2018. HDAC3 inhibition in diabetic mice may activate Nrf2 preventing diabetes-induced liver damage and FGF21 synthesis and secretion leading to aortic protection. *Am J Physiol Endocrinol Metab*, 315(2):E150-E162. https://doi.org/10.1152/ajpendo.00465.2017

Zhao B, Yuan Q, Hou JB, et al., 2019. Inhibition of HDAC3 ameliorates cerebral ischemia reperfusion injury in diabetic mice in vivo and in vitro. *J Diabetes Res*, 2019:8520856. https://doi.org/10.1155/2019/8520856

## 中文概要

**题　目：RGFP966 通过抑制 YAP 通路活化减轻长时程低温保存诱导的心功能损伤**

**目　的：**观察组蛋白脱乙酰化酶 3（HDAC3）抑制剂 RGFP966 是否能够促进低温保存心脏复灌期心功能的恢复，并探讨 Hippo-YAP 信号通路是否参与了 RGFP966 的心肌保护作用。

**创新点：**首次证实了在 Celsior 保存液中添加 RGFP966 可以减轻长时程低温保存引起的心脏功能障碍。该研究结果为临床实践中的心脏移植提供有价值且可行的策略，为患者获得远距供体心脏提供了可能。

**方　法：**将大鼠离体心脏置于含有或不含有 RGFP966 的 Celsior 保存液中低温保存 12 h 后，于 Langendorff 灌流系统中复灌 60 min，测定复灌期各项心功能指标。用 Western blotting 法分析 Mst1 和 YAP 蛋白表达和磷酸化水平。用 TUNEL 法测定心肌细胞凋亡情况。

**结　论：**RGFP966 可以促进低温保存心脏复灌期心功能的恢复，其作用机制可能是通过抑制 Hippo-YAP 信号传导通路的激活，增强心肌抗氧化能力，抑制心肌细胞凋亡而实现的。

**关键词：**低温保存；RGFP966；YAP；氧化应激；凋亡